Journal of Renewable
Energy and Environment

Journal Homepage: www.jree.ir

Aluminum Hydroxide-Based Flame-Retardant Composite Separator for Lithium-Ion Batteries

Ashkan Nahvi Bayani[a,b*], Mohammad Hadi Moghim[a,b], Saeed Bahadorikhalili[a], Abdolmajid Ghasemi[a]

[a] Department of Energy Storage, Institute of Mechanics, Shiraz, Iran.
[b] Department of Materials Science and Engineering, Engineering School, Shiraz University, Shiraz, Iran.

ABSTRACT

Despite the extensive use of polyolefins, especially in the form of lithium-ion battery (LIB) separators, their flammability limits their large-scale battery applications. Therefore, the fabrication of flame-retardant LIB separators has attracted much attention in recent years. In this work, composite separators were fabricated by applying a ceramic-based composite coating composed of a metal hydroxide as a filler and flame-retardant agent (Aluminium hydroxide, $Al(OH)_3$) and a binder (Poly(vinylidene Fluoride-co-hexafluoropropylene), P(VDF-HFP)) to the polypropylene (PP) commercial separator. Thermal shrinkage, thickness, air permeability, porosity, wettability, ionic conductivity, flame retardancy, and electrochemical performance of the fabricated ceramic-coated composite separator were investigated. The results showed that the addition of $Al(OH)_3$ particles improved thermal shrinkage ($\sim$8 %) and flame retardancy of the commercial separator, which can prevent dimensional changes at high temperatures and significantly increase LIBs safety. Applied 11 µm ceramic-based coating layer on PP commercial separator had 76 % porosity that increased the value of air permeability from 278.15 (s/100 cc air) to 312.8 (s/100 cc air), causing much facile air permeation through the pores of commercial separator than the composite one. Furthermore, suitable electrolyte uptake and the contact angle of ceramic coated separator (135 % and 91.19°, respectively) facilitated ion transport through the pores, which effectively improved the ionic conductivity of $Al(OH)_3$-coated PP separator (about 1.4 times higher than bare separator). Moreover, the cell comprising $Al(OH)_3$-coated PP separator had better cyclic performance than that of bare PP separator. All these characteristics make the fabricated flame-retardant $Al(OH)_3$ composite separator an appropriate candidate to ensure the safety of the large-scale LIB.

1. INTRODUCTION

By reducing fossil fuels and, thereby, increasing the importance of utilizing renewable energy sources, storage of electrical energy plays an essential role in improving the performance of power systems. There is much research and advancement in the realm of battery technology and fuel cells [1,2]; for this reason, different battery types such as vanadium redox [3,4] and lithium-based [5,6] have been developed over the past few decades. In recent years, the demand for high-performance rechargeable LIBs with excellent cycle life, energy, and safety has increased more than ever before [7]. Unlike the anodes and cathodes that have been extensively studied, the separator is the key component of LIBs for supplying their safety, which needs further investigation. The reason for this is the electrochemical inactivity of LIB separators [8]. However, it should be considered that large-scale LIBs, if not sufficiently safe, could threaten the consumer's life and lead to problems for battery manufacturers. The separator is the main component in ensuring safety of LIBs. The internal short circuits between the anode and the cathode can occur under abnormal conditions such as mechanical rupture, overcharging, and high-temperature storage that will lead to the explosion or production of fire and smoke, which is called the thermal runaway process [9]. Commercialized polyolefin separators, mainly polyethylene (PE) and polypropylene (PP), have relatively good properties. However, two major disadvantages that make them difficult to use in large-scale LIBs include deficient wettability and low melting temperature [10].

To enhance the safety of commercialized separators, two different approaches are implemented in the literature. These include separator surface coatings with high-temperature polymers such as polyimide or applying a layer of ceramic polymer composite to reduce thermal shrinkage and increase the flame retardancy of polyolefin separators.

So far, various studies have been done on composite separators fabricated by applying ceramic-based surface coatings (such as Titanium Oxide (TiO_2) [11] and Nickel Oxide (NiO) [12]) and heat-resistant polymers (such as Polyvinylidene Fluoride (PVDF) [13] and Polyimide (PI) [14]). Metal hydroxides, especially aluminum hydroxide ($Al(OH)_3$), act as filler, halogen-free flame retardant and smoke suppressant in polymeric materials by releasing water at high temperatures [15,16]. In general, Polypropylene (PP), as the substrate of composite separator in this work, has advantages such as small dielectric constant, good processability, and chemical stability [17]. However, due to its flammable properties, it is not suitable for use in large-scale LIBs. For these reasons, due to the higher decomposition temperatures than polyolefin separators, low cost, and environmental compatibility [18], metal hydroxides are considered as suitable additives for the preparation of fire-retardant composite separators in LIBs. However, few investigations have been performed on flame retardant ceramic-based composite separators for LIBs. In this research,

*Corresponding Author's Email: ashkan.nahvi@shirazu.ac.ir (A. Nahvi Bayani)

composite separators were prepared by applying a coating of flame-retardant $Al(OH)_3$ particles with P(VDF-HFP) as a binder on a commercial PP separator in order to enhance its flame retardancy properties in LIBs. Furthermore, thermal stability, wettability, gas permeability, porosity, ionic conductivity, and electrochemical performance of the prepared separator were also evaluated.

2. EXPERIMENTAL

2.1. Fabrication of a ceramic-based composite-coated separator

The coating solution was prepared by dissolving 1 wt. % P(VDF-HFP) (0.5 g, Kynar-Flex LBG, melting point=148-155 °C) for 3 h in acetone (45 g, 99.5 % purity, SAMCHUN CHEMICALS) and, then, dispersing 9 wt. % of $Al(OH)_3$ particles (4.5 g, MERCK, density=2.42 g/cm³, average particle size ≅ 90μm) by vigorous magnetic stirring for 24 h at room temperature. The weight ratio of ceramic/P(VDF-HFP) was fixed at 9/1 by weight. Commercial PP separator (42±3 % porosity, 21 μm thickness) was soaked in $Al(OH)_3$-based slurry solution for 5 min by immersion method. The Immersed separator was then dried in a conventional oven at 60 °C for 18h to prepare for further characterizations.

2.2. Characterization

The surface morphology of the commercial and $Al(OH)_3$-coated PP separators was investigated by scanning electron microscopy (SEM, MIRA3 TESCAN). For this purpose, the commercial and coated separators were attached to the sample holder and gold coating was applied to increase the electronic conductivity. Separator thickness was measured with a digital micrometer of 0.001 mm precision.

Thermal shrinkage of bare and composite separators was evaluated by measuring their area-based dimensional changes cut into squares (4 cm×4 cm) after subjection to heat treatment at 130 °C and 150 °C for 1 h. Thermal shrinkage is calculated according to Equation (1):

$$\text{Thermal Shrinkage (\%)}=\left(\frac{[A_f - A_i]}{A_i}\right)\times 100 \qquad (1)$$

where A_i and A_f are the samples' area before and after heat treatment process, which were measured by ImageJ [19] image processing software. Moreover, the water release test of $Al(OH)_3$ (1 g) was done by exposing it at high temperatures in a conventional oven ranging from 180 to 220 °C. The amount of released water was evaluated according to the following equation:

$$\text{Released Water (Wt \%)}=\left(\frac{[W_1 - W_2]}{W_1}\right)\times 100 \qquad (2)$$

where W_1 and W_2 are the weights of $Al(OH)_3$ before and after heating. Flame-retardant behavior of bare and composite separators was also examined by the ignition of separators by setting them on fire.

Air permeability was obtained using Gurley Analyzer by measuring the time necessary for a determined volume of air (100 cc) to pass through the separator under a given pressure [20].

Porosity of composite coating was evaluated according to Equation (3) [21]:

$$\text{Porosity of composite Coating (\%)} =$$
$$\frac{\text{(Volume of composite Coating-True volume of composite Coating)}}{\text{Volume of composite Coating}} =$$
$$\frac{(A\times t)-w\left(r_c\times d_c+r_p\times d_p\right)^{-1}}{(A\times t)} \qquad (3)$$

where A is the composite separator's area; t and w are the thickness and weight of composite coating, respectively. r_c and r_p are the ratios of $Al(OH)_3$ particles (0.9) and P(VDF-HFP) binder (0.1), respectively. d_c and d_p are the true density of $Al(OH)_3$ particles (2.42 g.cm⁻³) and P(VDF-HFP) binder (1.77 g.cm⁻³), respectively.

Electrolyte uptake of bare and composite separators was assessed by measuring their weights before and after soaking in LIB electrolyte (1 M $LiPF_6$ solution in a mixture of EC/DMC (1:1)) for 1 h using Equation (4):

$$\text{Electrolyte Uptake (\%)}=\left(\frac{[W_2 - W_1]}{W_1}\right)\times 100 \qquad (4)$$

where W_1 and W_2 represent weights of the separators before and after soaking in LIB electrolyte, respectively. Contact angles (CA), a major indicator of wettability, were measured by contact angle goniometer. A water droplet around 5 μL was released from a needle tip onto the surface of bare and coated separators. A motion camera was mounted to capture the images, and contact angles were analyzed with the aid of specific software.

Ionic conductivity was measured by electrochemical impedance spectroscopy (EIS) of a split test cell (MTI corp.) assembled with the bare and coated separators immersed in LIB electrolyte (1M $LiPF_6$ solution in a mixture of EC/DMC (1:1)) and sandwiched between two stainless steel electrodes (1.6 cm in diameter). The assembled cell was kept for 24 hours within a dry argon-filled glove-box to be saturated with electrolyte without electrochemical reaction. AC impedance measurements were carried out in the frequency range of 100 mHz to 100 kHz at 25 °C at a 5 mV scan rate using an impedance analyzer. Consequently, ionic conductivity (σ) can be obtained through the following equation:

$$\sigma=\frac{l}{R_b A} \quad (\text{S cm}^{-1}) \qquad (5)$$

where l and A are the thickness and contact area of the separators, respectively, and R_b is the bulk resistance obtained through AC impedance test.

In order to evaluate the battery performance, 2025 type lithium-ion coin cells were assembled using bare and $Al(OH)_3$-coated PP separators. The cyclic performance of $LiCo_{0.15}Ni_{0.8}Al_{0.05}O_2$/bare and coated separators/Artificial Graphite (AGP) was examined using a battery test system at room temperature.

3. RESULTS AND DISCUSSION

3.1. Surface morphology

In this research, a dry process manufactured polypropylene separator was used as a coating substrate for the production of composite separators (Figure 1(a)). According to the surface morphology of coated separator shown in Figure 1(b), fine interconnected pores are dispersed uniformly throughout the fixed ratio of $Al(OH)_3$ particles and P(VDF-HFP) binder applied to both sides of the substrate by an automatic coating machine. In addition, SEM images show that the PP substrate

is successfully covered by a homogeneous layer of ceramic and binder mixture after coating and drying of the ceramic slurry on both surface of the commercial separator. A different surface morphology and pore structures of the $Al(OH)_3$-coated PP separator can affect the porosity and air permeability of the substrate, to be discussed further below.

(a)

(b)

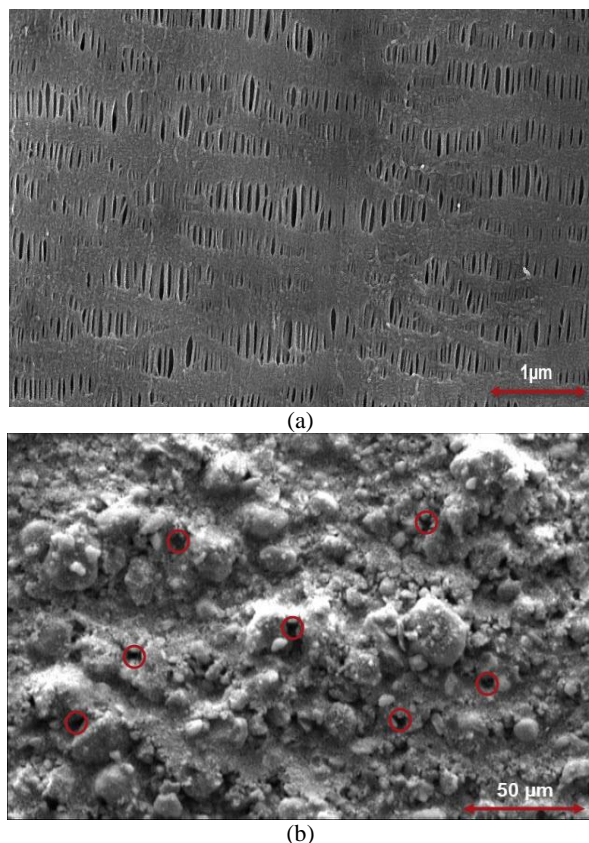**Figure 1.** SEM images of a) bare PP and b) $Al(OH)_3$-coated PP separators. Red circles in image (b) indicate some of the fine interconnected pores dispersed uniformly throughout the coating.

3.2. Water release test

In order to evaluate the flame-retardant behavior of aluminium hydroxide-based composite separators, water release test is an effective technique. The endothermic decomposition of aluminum hydroxide to aluminum oxide and, subsequently, the release of water during heating between 180 to 220 °C are the main reasons for improving the flame-retardant properties of the aluminium hydroxide-based composite separator. Figure 2 shows the water release of $Al(OH)_3$ at various temperatures between 180 °C and 220 °C. The results showed that chemically-combined water in $Al(OH)_3$ structure was released even at 180 °C (0.45 wt. %); however, the amount of released water significantly increased at 200 °C (1.72 wt. %). As shown in Equation (6), these results are compatible with flame-retardant nature of metal hydroxides and their decomposition at high temperatures associated with the release of water [22]:

$$2Al(OH)_{3\ solid} \rightarrow Al_2O_{3\ solid} + 3H_2O_{gas}\ (1050\ kJ/kg) \qquad (6)$$
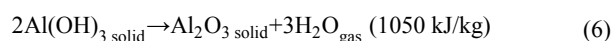
According to reported pieces of literature, aluminum hydroxide weight loss below 200 °C is mainly related to absorbed water molecules on the surface of hydroxide particles, while thermal decomposition begins at about 200 °C [22-24]. Based on the presented results in this section,

$Al(OH)_3$ seems suitable for use as a flame-retardant agent in composite LIB separators.

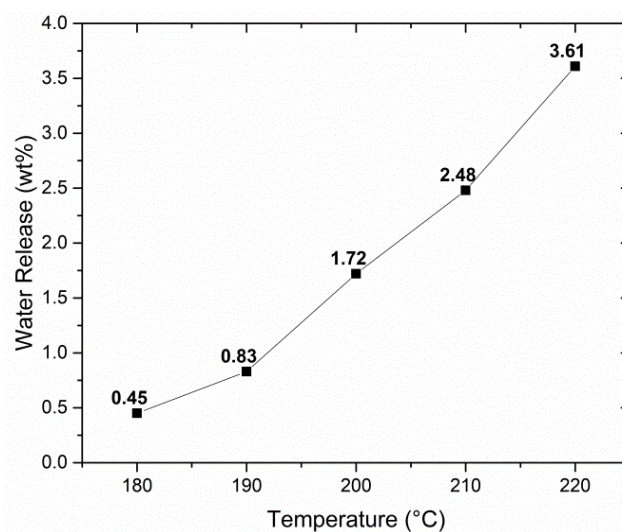**Figure 2.** Effect of temperature on water release amount of $Al(OH)_3$ after 30 min heating exposure.

3.3. Thermal stability

Due to exothermic reactions occurring during the process of LIB charging and discharging, the separator should have high thermal stability in order to ensure battery safety. The amount of released heat can lead to the deformation of the separator and even short circuit of the battery, which can locally increase the temperature and cause flame, smoke, and explosion. Thermal shrinkage of composite separators can be calculated by measuring the surface area changes after their heat treatment at various temperatures. Figure 3 presents the thermal shrinkage of bare and composite $Al(OH)_3$-coated PP separators at 130 and 150 °C for 60 min. As shown in Figure 3, the thermal shrinkage of both separators increases by increasing of temperature. At 150 °C, the bare PP separator and the composite one show the shrinkage of 38.6 % and 31.4 %, respectively. Improved thermal stability of the composite separator results from the addition of $Al(OH)_3$ particles. The heat-resistant $Al(OH)_3$ particles effectively prevent the composite separator from being thermally shrunk. Attached photographs in Figure 3 show the surface area changes of bare and composite separators before and after exposure to various temperatures. The values of thermal shrinkages of bare and composite separators are given in Table 1. All these results show that the addition of inorganic $Al(OH)_3$ successfully has improved the safety of LIBs. Therefore, it can be expected that using the $Al(OH)_3$-coated PP separators will increase the thermal stability and safety of LIBs.

3.4. Air permeability

Gurley number, which is defined as the time required for passing a specific amount of air through a specific area of a separator under a given pressure, is a measure of air permeability. The bare PP separator exhibited a smaller Gurley number (288.6 s/100 cc air) than the $Al(OH)_3$-coated PP separator (312.8 s/100 cc air), which can be attributed to the easier permeation of air through the porosity of the bare PP separator. The presence of a ceramic coating layer with thickness of 11 μm and blocking the air path toward the pores makes the results sensible. However, the relatively small

difference between the Gurley number of bare and composite separators shows that the ceramic-based composite coating does not have much effect on the air permeability of the bare PP separator.
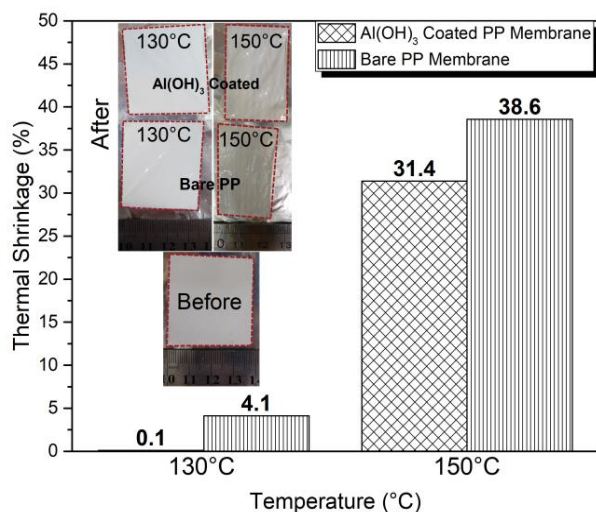

Figure 3. Thermal shrinkage of bare and Al(OH)₃-coated PP separators at 130 and 150 °C. The inset image shows the separators after exposure to various temperatures for 60 min.

**Table 1.** General properties of bare and Al(OH)₃-coated PP separators.

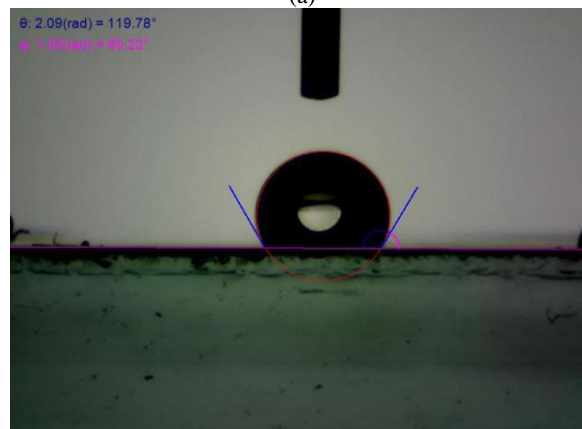|	**Bare PP separator**	**Al(OH)₃-coated PP separator**
Thickness (μm)	21	32
Gurley no. (s/100 cc air)	288.6	312.8
Electrolyte uptake (%)	70	135
Contact angle (°)	119.78	91.19
Coating layer porosity (%)	....	76
Thermal shrinkage @ 130 °C (%)	4.1	~0
Thermal shrinkage @ 150 °C (%)	38.6	31.4

3.5. Wettability

The wettability of battery separators is one of the most important parameters for the electrochemical performance of LIBs, affected by surface chemistry and pore structure of the separators and characterized by electrolyte uptake and contact angle analysis. Separators with good wettability can effectively retain the liquid electrolyte and facilitate ionic transportation between the electrodes [25].

Electrolyte uptake of bare and Al(OH)₃-coated PP separators was evaluated by measuring their weights before and after soaking in LIB electrolyte for 1 h. According to the previous studies, electrolyte uptake of polyolefin separators depends on their porosity and surface wettability [9,26]. Therefore, Al(OH)₃-coated PP separator exhibited higher electrolyte uptake (135 %) than bare PP separator (70 %). Since the polyolefin-based separators such as those comprising PE and PP are naturally hydrophobic and cannot be easily wetted by polar liquid electrolytes with a high dielectric constant, the application of a hydrophilic Al(OH)₃ layer improved the wettability and electrolyte uptake of bare PP separator because of the presence of oxygen atoms. The electrolyte wettability of the bare and Al(OH)₃-coated PP separators is shown in Figure 4(a). The liquid electrolyte droplet was easily spread into a

larger area of the composite separator surface, while the bare PP separator was not uniformly wetted at the same time due to its lower electrolyte Uptake and absorption rate than the Al(OH)₃-coated PP separator. This remarkable wetting behavior of composite separator and, thus, filling the separator pores from the liquid electrolyte made the Al(OH)₃-coated PP separator transparent, while the bare PP separator looked opaque. Figures 4(b) and (c) show contact angles of bare and coated separators. The lower contact angle leads to greater wettability of the separator surface. Contact angles of bare and Al(OH)₃-coated PP separators are 119.78° and 91.19°, respectively (Table 1). As expected, the presence of hydrophilic Al(OH)₃ particles on the surface of the coated separator decreased the contact angle of water that can accelerate the wetting of Al(OH)₃-coated PP separator in LIBs. Therefore, Al(OH)₃ particles were used successfully to change bare PP separator surface to much hydrophilic surface. The electrolyte uptake amount and contact angles of bare and Al(OH)₃-coated PP separators are summarized in Table 1.
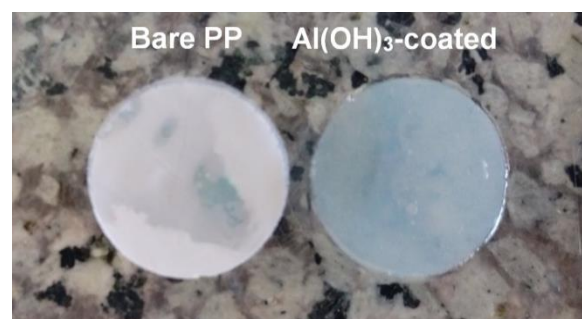
(a)

(b)
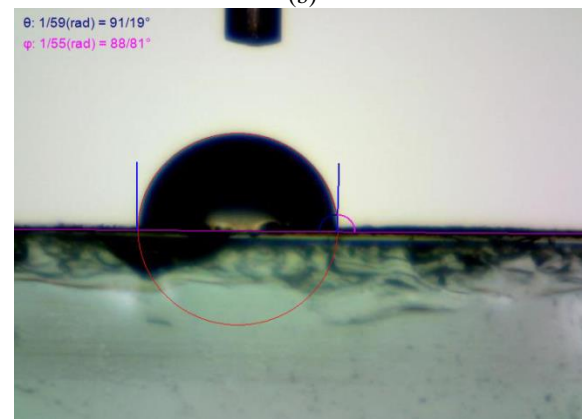
(c)

Figure 4. Wettability comparison of bare and Al(OH)₃-coated PP separators with one droplet of liquid electrolyte (a), contact angle measurement on Bare PP (b), and Al(OH)₃-coated PP separators (c).

3.6. Flame retardancy

Figure 5 shows the combustion tests of bare and composite separators. The commercial PP separator shrank immediately after being exposed to the fire and ignited after 5 seconds. This is due to the combustible nature of polyolefin separator. Hopefully, Al(OH)$_3$-coated PP separator exhibited perfect flame retarding and smoke suppression ability. As shown in Figure 5, the composite separator retained its dimensions after 5 seconds of exposure to the fire and required more time to shrink (10 seconds). Furthermore, unlike the bare PP separator, it did not catch fire despite shrinking. Therefore, the results showed that the application of a ceramic-based coating layer comprising Al(OH)$_3$ as a filler and flame-retardant agent and a P(VDF-HFP) binder to PP commercial separator could significantly increase the flame-retarding ability of commercial separators and improve the safety of LIBs.
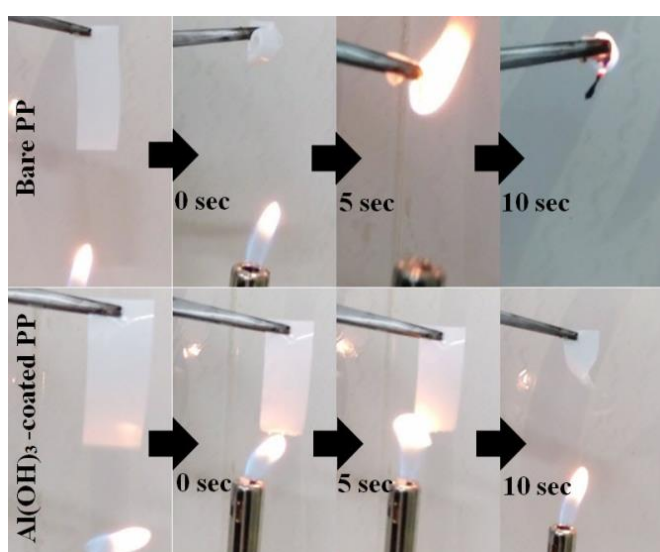

Figure 5. Combustion tests of bare and Al(OH)$_3$-coated PP separators after 0, 5, and 10 seconds.

3.7. Ionic conductivity

The Nyquist curves of bare and Al(OH)$_3$-coated PP separators obtained by electrochemical impedance spectroscopy (EIS) at 25 °C are shown in Figure 6. Both Nyquist curves show inclined straight lines at high frequencies, which can be observed from the inset image of Figure 6. The interception of straight lines with real axes (z') indicates ionic resistance of bare and Al(OH)$_3$-coated PP separators, which can be used to calculate ionic conductivity of separators through Equation (5). Bulk resistance and ionic conductivity of separators are summarized in Table 2.

The presence of a ceramic-based composite coating layer on the surface of separators can significantly influence their ionic conductivity. The ionic conductivity of bare and Al(OH)$_3$-coated PP separators is 0.29 and 0.41 mS.cm^{-1}, respectively, which can be concluded that the application of a layer of Al(OH)$_3$ results in an increase in the ionic conductivity of the bare PP separator up to 1.4 times. On the one hand, this ceramic layer increases the penetration path of the lithium ions between the anode and the cathode, and the attendance of pores in this coating layer hampers the conduction of Li$^+$. Intensive Al(OH)$_3$ particles can also reduce the boundary resistance of the separator. Moreover, the application of a ceramic coating layer can create the charge field that will interact with the liquid electrolyte to form a double layer

charge. According to the results shown in Table 1, the presence of ceramic coating significantly improved the electrolyte uptake and surface contact angle of the bare separator, which can have a great effect on improving the ionic conductivity of the Al(OH)$_3$-coated PP separator [27-29].
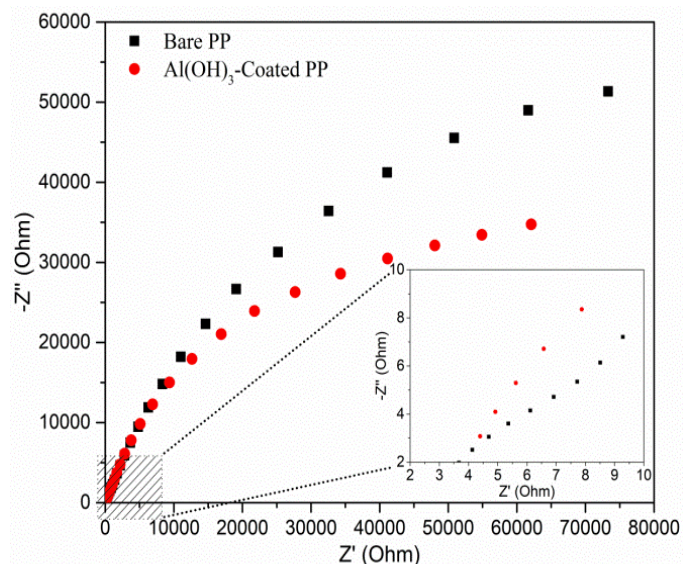

Figure 6. Electrochemical impedance spectroscopy (EIS) curves for bare and Al(OH)$_3$-coated PP separators. The inset image shows inclined straight lines of Nyquist Curves at high frequencies.

Table 2. Required parameters for the calculation of separators' ionic conductivity.

	Thickness (cm)	Contact area (cm^2)	Bulk resistance (Ω)	Ionic conductivity (mS.cm^{-1})
Bare PP separator	0.0021	2.01	3.61	0.29
Al(OH)$_3$-coated PP separator	0.0032	2.01	3.92	0.41

3.8. Electrochemical performance

The effect of Al(OH)$_3$ /P(VDF-HFP) on the charge-discharge behavior of the bare PP separator is illustrated in Figure 7. As can be seen from the specific discharge capacity vs. cycle number diagram, an increase in the number of cycles is observed, which is associated with a decrease in the specific capacity of the cell. The initial specific discharge capacities of the cells with bare and Al(OH)$_3$-coated PP separators are approximately equal to each other, which are higher than the result reported by Yeon et. al [21]. The cell comprising Al(OH)$_3$-coated PP separator has better cyclic performance than that of the bare PP separator. The Al(OH)$_3$ ceramic-coated separator retains 74 % of the initial discharge capacity, whereas the bare PP separator retains 66.8 % of the initial capacity. Although increasing the penetration path of lithium ions and becoming more difficult to migrate between the cathode and the anode can lead to the reduced discharge capacity; however, Al(OH)$_3$ coating with P(VDF-HFP) binder on the bare PP separator improves capacity retention after 100 cycles, which may be due to increased electrolyte uptake and wettability of the coated separator than the bare one [30,31].
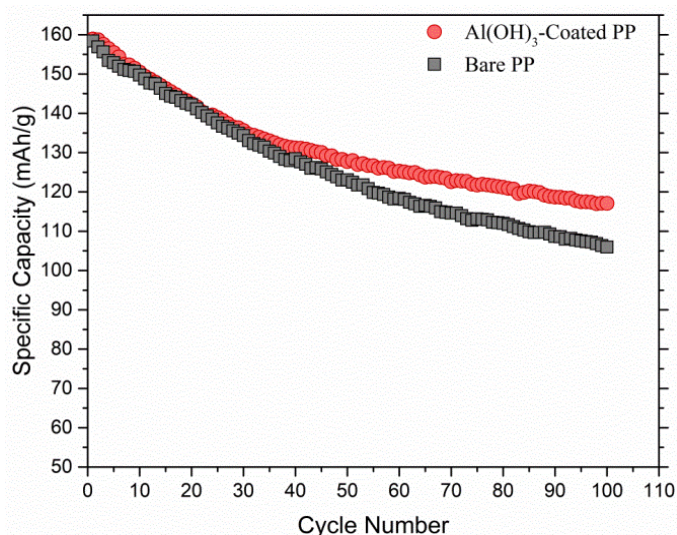
Figure 7. Cyclic performance of coin cells assembled with bare and Al(OH)₃-coated PP separators.

4. CONCLUSIONS

In this paper, Al(OH)$_3$-coated PP separator was successfully fabricated via the immersion method for LIB application. The prepared composite separator showed high thermal stability, better wettability, improved ionic conductivity and cyclic performance, and superior flame retardancy compared to the bare commercial PP separator because of their released water at high temperatures. Improvement of the Al(OH)$_3$-coated PP separator in thermal stability, ionic conductivity, wettability, and electrochemical performance resulted from the presence of heat-resistant and hydrophilic Al(OH)$_3$ particles, which significantly increased the safety of LIBs. All these specifications made the fabricated Al(OH)$_3$-coated PP separator a promising candidate to ensure the safety of large-scale high-performance rechargeable LIBs.

5. ACKNOWLEDGEMENT

REFERENCES

1. Sarirchi, S. and Rowshanzamir, S., "An overview of organic/inorganic membranes based on sulfonated poly ether ether ketone for application in proton exchange membrane fuel cells", *Journal of Renewable Energy and Environment (JREE)*, Vol. 4, (2017), 46-60.

2. Ahmadi, N., Rezazadeh, S.A. and Dadvand, A., "Numerical investigation of the effect of gas diffusion layer with semicircular prominences on polymer exchange membrane fuel cell performance and species distribution", *Journal of Renewable Energy and Environment (JREE)*, Vol. 2, (2015), 36-46.

3. Moghim, M.H., Eqra, R., Babaiee, M., Zarei-Jelyani, M. and Loghavi, M.M., "Role of reduced graphene oxide as nano-electrocatalyst in carbon felt electrode of vanadium redox flow battery", *Journal of Electroanalytical Chemistry*, Vol. 789, (2017), 67-75. (https://doi.org/10.1016/j.jelechem.2017.02.031).

4. Zarei-Jelyani, M., Babaiee, M., Ghasemi, A. and Eqra, R., "Investigation of hydroxylated carbon felt electrode in vanadium redox flow battery by using optimized supporting electrolyte", *Journal of Renewable Energy and Environment (JREE)*, Vol. 3, (2016), 54-59.

5. Loghavi, M.M., Askari, M., Babaiee, M. and Ghasemi, A., "Improvement of the cyclability of Li-ion battery cathode using a chemical-modified current collector", *Journal of Electroanalytical Chemistry*, Vol. 841, (2019), 107-110. (https://doi.org/10.1016/j.jelechem.2019.04.037).

6. Raja, M., Angulakshmi, N., Thomas, S., Kumar, T.P. and Stephan, A.M., "Thin, flexible and thermally stable ceramic membranes as separator for lithium-ion batteries", *Journal of Membrane Science*, Vol. 471, (2014), 103-109. (https://doi.org/10.1016/j.memsci.2014.07.058).

7. Guo, Y.-G., Hu, J.-S. and Wan, L.-J., "Nanostructured materials for electrochemical energy conversion and storage devices", *Advanced Materials*, Vol. 20, (2008), 2878-2887. (doi:10.1002/adma.200800627).

8. Kim, J.-H., Kim, J.-H., Choi, K.-H., Yu, H.K., Kim, J.H., Lee, J.S. and Lee, S.-Y., "Inverse opal-inspired, nanoscaffold battery separators: A new membrane opportunity for high-performance energy storage systems", *Nano Letters*, Vol. 14, (2014), 4438-4448. (doi:10.1021/nl5014037).

9. Arora, P. and Zhang, Z., "Battery separators", *Chemical Reviews*, Vol. 104, (2004), 4419-4462. (doi:10.1021/cr020738u).

10. Abraham, K.M., Alamgir, M. and Hoffman, D.K., "Polymer electrolytes reinforced by Celgard® Membranes", *Journal of The Electrochemical Society*, Vol. 142, (1995), 683-687.

11. Chen, H., Lin, Q., Xu, Q., Yang, Y., Shao, Z. and Wang, Y., "Plasma activation and atomic layer deposition of TiO$_2$ on polypropylene membranes for improved performances of lithium-ion batteries", *Journal of Membrane Science*, Vol. 458, (2014), 217-224. (https://doi.org/10.1016/j.memsci.2014.02.004).

12. Prasanna, K., Subburaj, T., Lee, W.J. and Lee, C.W., "Polyethylene separator: Stretched and coated with porous nickel oxide nanoparticles for enhancement of its efficiency in Li-ion batteries", *Electrochimica Acta*, Vol. 137, (2014), 273-279. (https://doi.org/10.1016/j.electacta.2014.06.026).

13. Lee, Y.M., Kim, J.-W., Choi, N.-S., Lee, J.A., Seol,W.-H. and Park, J.-K., "Novel porous separator based on PVdF and PE non-woven matrix for rechargeable lithium batteries", *Journal of Power Sources*, Vol. 139, (2005), 235-241. (https://doi.org/10.1016/j.jpowsour.2004.06.055).

14. Song, J., Ryou, M.-H., Son, B., Lee, J.-N., Lee, D.J., Lee, Y.M., Choi, J.W. and Park, J.-K., "Co-polyimide-coated polyethylene separators for enhanced thermal stability of lithium ion batteries", *Electrochimica Acta*, Vol. 85, (2012), 524-530. (https://doi.org/10.1016/j.electacta.2012.06.078).

15. Jiao, C.M. and Chen, X.L., "Flame retardant synergism of hydroxy silicone oil and Al(OH)$_3$ in EVA composites", *Polymer-Plastics Technology and Engineering*, Vol. 48, (2009), 665-670. (doi:10.1080/03602550902824531).

16. Ramazani, S.A.A., Rahimi, A., Frounchi, M. and Radman, S., "Investigation of flame retardancy and physical-mechanical properties of zinc borate and aluminum hydroxide propylene composites" *Materials & Design*, Vol. 29, (2008), 1051-1056. (https://doi.org/10.1016/j.matdes.2007.04.003).

17. Liang, J.-Z., "Toughening and reinforcing in rigid inorganic particulate filled poly(propylene): A review", *Journal of Applied Polymer Science*, Vol. 83, (2001), 1547-1555. (doi:10.1002/app.10052).

18. Shabanian, M. and Ghanbari, D., "Synthesis of magnesium hydroxide nanofiller and its use for improving thermal properties of new poly(ether-amide)", *Journal of Applied Polymer Science*, Vol. 127, (2012), 2004-2009. (doi:10.1002/app.37640).

19. https://imagej.nih.gov/ij/.

20. Yu, L., Jin, Y. and Lin, Y.S., "Ceramic coated polypropylene separators for lithium-ion batteries with improved safety: Effects of high melting point organic binder", *RSC Advances*, Vol. 6, (2016), 40002-40009. (doi:10.1039/C6RA04522G).

21. Yeon, D., Lee, Y., Ryou, M.-H. and Lee, Y.M., "New flame-retardant composite separators based on metal hydroxides for lithium-ion batteries", *Electrochimica Acta*, Vol. 157, (2015), 282-289. (https://doi.org/10.1016/j.electacta.2015.01.078).

22. Sain, M., Park, S.H., Suhara, F. and Law, S., "Flame retardant and mechanical properties of natural fibre–PP composites containing magnesium hydroxide", *Polymer Degradation and Stability*, Vol. 83, (2004), 363-367. (https://doi.org/10.1016/S0141-3910(03)00280-5).

23. Zhang, A., Zhang, Y., Lv, F. and Chu, P.K., "Synergistic effects of hydroxides and dimethyl methylphosphonate on rigid halogen-free and flame-retarding polyurethane foams", *Journal of Applied Polymer Science*, Vol. 128, (2012), 347-353. (doi:10.1002/app.38200).

24. Sato, T., "Thermal decomposition of aluminium hydroxides to aluminas", *Thermochimica Acta*, Vol. 88, (1985), 69-84. (https://doi.org/10.1016/0040-6031(85)85415-0).

25. Zhang, S.S., "A review on the separators of liquid electrolyte Li-ion batteries", *Journal of Power Sources*, Vol. 164, (2007), 351-364. (https://doi.org/10.1016/j.jpowsour.2006.10.065).

26. Lee, Y., Ryou, M.-H., Seo, M., Choi, J.W. and Lee, Y.M., "Effect of polydopamine surface coating on polyethylene separators as a function of their porosity for high-power Li-ion batteries", *Electrochimica Acta*, Vol. 113, (2013), 433-438. (https://doi.org/10.1016/j.electacta.2013.09.104).

27. Zhang, Z., Lai, Y., Zhang, Z., Zhang, K. and Li, J., "Al_2O_3-coated porous separator for enhanced electrochemical performance of lithium sulfur batteries", *Electrochimica Acta*, Vol. 129, (2014), 55-61. (https://doi.org/10.1016/j.electacta.2014.02.077).

28. Xu, R., Lin, X., Huang, X., Xie, J., Jiang, C. and Lei, C., "Boehmite-coated microporous membrane for enhanced electrochemical performance and dimensional stability of lithium-ion batteries", *Journal of Solid State Electrochemistry*, Vol. 22, No. 3, (2017), 739-747. (doi:10.1007/s10008-017-3780-3).

29. Wang, Z.,Xiang, H., Wang, L., Xia, R., Nie, S., Chen, C. and Wang, H., "A paper-supported inorganic composite separator for high-safety lithium-ion batteries", *Journal of Membrane Science*, Vol. 553, (2018), 10-16. (https://doi.org/10.1016/j.memsci.2018.02.040).

30. Shi, C., Dai, J., Shen, X., Peng, L., Li, C., Wang, X., Zhang, P. and Zhao, J., "A high-temperature stable ceramic-coated separator prepared with polyimide binder/Al_2O_3 particles for lithium-ion batteries", *Journal of Membrane Science*, Vol. 517, (2016), 91-99. (https://doi.org/10.1016/j.memsci.2016.06.035).

31. Jeon, H., Yeon, D., Lee, T., Park, J., Ryou, M.-H. and Lee, Y.M., "A water-based Al_2O_3 ceramic coating for polyethylene-based microporous separators for lithium-ion batteries", *Journal of Power Sources*, Vol. 315, (2016), 161-168. (https://doi.org/10.1016/j.jpowsour.2016.03.037).